Spectrochimica Acta Part B: Atomic Spectroscopy 235 (2026) 107356

Contents lists available at ScienceDirect

Spectrochimica Acta Part B: Atomic Spectroscopy

journal homepage: www.elsevier.com/locate/sab

Improved detection capabilities of molecular emission in microwave-enhanced laser-induced plasma

L. García-Gómez [a], J.K. Soriano [b], J.M. Vadillo [a,c,*], Y. Ikeda [b,*]

[a] UMALASERLAB, Departamento de Química Analítica, Universidad de Málaga, Jiménez Fraud 4, 29010 Málaga, Spain
[b] i-Lab., Inc., #213 KIBC Bldg., 5-5-2 Minatojima-Minami, Chuo, Kobe 650-0047, Japan
[c] Instituto Universitario de Materiales y Nanotecnología (IMANA), University of Málaga, 29071, Málaga, Spain

ARTICLE INFO

Keywords:
LIBS
MW-LIBS
re-excitation
molecular emission

ABSTRACT

The detection of molecular emissions in laser-induced breakdown spectroscopy (LIBS) remains a subject of active research, driven by the need to improve both signal-to-noise ratios and spectral definition. Various enhancement strategies have been proposed, including double-pulse configurations and hybrid systems combining LIBS with complementary techniques like Raman spectroscopy or laser-induced fluorescence. While effective, these methods often introduce considerable experimental complexity. In this context, the present study explores microwave re-excitation (MW-LIBS) as a more accessible alternative capable of modifying plasma dynamics without additional optical alignment. The introduction of microwave energy increases collisional activity within the plasma, extending its duration to the millisecond range and amplifying emission signals. Molecular species were monitored under this regime, focusing on canonical emitters such as CN and CaO, as well as less commonly reported systems like SnO, which has not been previously described in LIBS literature. The most significant enhancements were observed under conditions approaching the plasma ablation threshold. Moreover, MW-LIBS enabled the observation of molecular emissions in the red and near-infrared regions, which are generally limited in conventional LIBS due to detector inefficiencies and reduced plasma radiative output. These findings provide new insights into the mechanisms of molecular formation in sustained plasmas and demonstrate the potential of MW-LIBS for enhancing molecular diagnostics.

1. Introduction

Laser-induced breakdown spectroscopy (LIBS) is a widely applied analytical technique known for its versatility and speed [1–4]. Nevertheless, efforts continue to enhance its performance, particularly in terms of sensitivity, where improvements aim to refine detection limits and signal quality [5]. In LIBS, a high-intensity laser pulse is focused onto the target surface, generating a plasma composed of electrons, atoms, ions, and transient molecular fragments derived from the ablated material. The emission characteristics of this plasma are governed by the efficiency of three interconnected processes: a) ablation, which controls the amount of material vaporized; b) atomization, which determines the fraction of atoms liberated from the condensed phase; and c) excitation, which defines the proportion of neutral species promoted to excited/radiative states. These parameters collectively rule the spectral intensity and analytical usefulness of the signal.

A laser-induced plasma is inherently a non-stationary entity whose physicochemical properties evolve continuously from the moment of its formation. During the initial stages, the plasma exhibits elevated electron temperatures and densities, resulting in an emission regime dominated by continuum radiation (produced by inverse bremsstrahlung) and by broadened ionic lines. This phase of the plasma lifetime corresponds to the maximum photon yield, although its spectral content is largely non-specific and limits analytical resolution [6]. As plasma expands and undergoes radiative and collisional energy losses, processes such as recombination and relaxation reduce the degree of ionization, giving rise to useful narrower neutral atomic emissions at the cost of a lower overall emission. In the later stages of plasma evolution, molecular emissions may also be detected, since excited species in the plasma can react with each other to form more complex diatomic species. This temporal evolution of the plasma affects not only the spectral features and the optimal timing for data acquisition in LIBS [7], but also encourages the development of alternative strategies aimed at increasing the signal-to-noise ratio (SNR) either by extending plasma lifetime after

* Corresponding authors.
E-mail addresses: jmvadillo@uma.es (J.M. Vadillo), yuji@i-lab.net (Y. Ikeda).

https://doi.org/10.1016/j.sab.2025.107356
Received 25 June 2025; Received in revised form 7 October 2025; Accepted 7 October 2025
Available online 8 October 2025

the decay of the continuum, by increasing the ablation rate to raise the number of species present in plasma, or by selective enhancing the emission.

One of the most effective strategies has been the use of multi-pulse configurations, such as double-pulse LIBS (DP-LIBS) and multiple-pulse LIBS (MP-LIBS). These approaches increase energy deposition through the sequential delivery of laser pulses, significantly impacting signal enhancement [8,9]. The spatial configuration of the laser pulses, whether collinear, cross-beam, or orthogonal, also plays an important role in the effectiveness of SNR improvement [10,11]. However, these configurations introduce additional challenges, including pulse overlap, synchronization issues, and the need for precise optimization of parameters such as inter-pulse delay. While most studies focus on the enhancement of atomic and ionic emissions, research on improving molecular signals is less extensive [8], as the mechanisms responsible for the enhancement are less effective in this case [12]. It has been suggested in the literature that this effect may be attributed to the increase in plasma temperature caused by the double-pulse configuration, which could lead to a higher rate of molecular dissociation [12].

Regarding the enhancement of molecular information or signals, various approaches have been explored, such as the combination of LIBS with complementary spectroscopic methods like laser-induced fluorescence (LIF-LIBS) [13–15]. LIF-LIBS enhances species identification by selectively stimulating molecules to higher energy states. This process significantly increases the population of particles at the corresponding upper state [16].

One of the limitations of LIF-LIBS is that it restricts excitation to specific spectral regions, as each laser wavelength preferentially excites a particular species. This limitation restricts the excitation of the entire spectral range and limits its applicability to all species [16,17]. Consequently, LIF-LIBS enhances only a specific transition of a single element per spectrum, therefore, it is less suitable for broadband spectral analysis. Likewise, it requires the use of tunable lasers, which implies greater instrumental complexity and precise wavelength stabilization to ensure resonance with the desired transition. Another important factor is the quenching effect, which can be problematic under atmospheric pressure and in environments with high oxygen content. As a result, LIF-LIBS performs better in controlled, low-pressure atmospheres with inert gases like argon. However, working in such controlled conditions can be experimentally challenging, adding complexity to the setup [18,19].

An alternative approach, microwave-assisted laser-induced breakdown spectroscopy (MW-LIBS), has been proposed to address some of these limitations of existing methods, especially in the context of molecular emission signal enhancement. This system employs microwave radiation to re-excite the plasma after it is initially formed by a laser pulse. This re-excitation process increases the number of effective collisions within the plasma, which prolongs its duration up to several milliseconds and enhances emission intensities. MW-LIBS not only amplifies signal strength but also improves SNR. These features reflect a substantial enhancement of the interactions between the plasma and the surrounding atmosphere, which can strongly influence the persistence, evolution, and formation of molecular species. The extended plasma duration, combined with its expanded spatial domain, provides a more favorable environment for gas-phase reactions, including recombination processes and the stabilization of molecular fragments that are typically disrupted in the early stages of plasma evolution [20].

In the framework of this study, the spectral behavior of different molecular species, including CN, CaO, and SnO, was investigated under varying laser energy conditions. In particular, experiments focusing on the violet emission of the CN system $B^2\Sigma^+ \rightarrow X^2\Sigma^+$ at 358.4 nm revealed that the signal intensity reached its maximum near the plasma formation threshold. However, the magnitude of the enhancement factor varied among the different molecules, underscoring the need for an individualized examination of their formation mechanisms.

Despite the preliminary nature of the results, a systematic improvement in detection was observed for all species tested when microwave re-excitation was applied. These findings support the potential of MW-LIBS as a versatile technique for the enhancement of molecular signals, opening new perspectives for its application in diverse analytical contexts and in samples of different natures.

2. Set up and methodology

2.1. MW-LIBS set up

The experimental setup, depicted in Fig. 1, was employed for all LIBS and MW-LIBS measurements. A Q-switched Nd: YAG laser (Big Sky, 1064 nm, 8 ns pulse width, 15 Hz) was used to generate plasmas by focusing the beam onto the sample using a plano-convex quartz lens (10 cm focal length). Laser energy adjustments were achieved by a combination of an absorption green filter with an optical density of 1.21 at 1064 nm and control of the laser Q-switch delay values. With this configuration, reproducible control was achieved across all energy ranges used.

A single-pulse microwave, with a peak-to-peak power of 1.0 kW and a duration of 1.0 ms (energy delivered during the pulse 1 J), was synchronously coupled with the laser pulse that acts as a master trigger for the MW generator, ensuring a good synchronization. Microwaves were operated at 2.45 GHz under TTL-like modulation. The microwave antenna consisted of a copper helical coil with a length of 4.5 cm and a diameter of 0.5 mm [21]. A 3-stub tuner was employed to match the impedance of the microwave system. An oscilloscope was used to monitor both the laser synchronization and the reflected and transmitted microwaves during the experiment.

Plasma emission was collected perpendicularly (90°) using a fused-silica lens (60 mm focal length) and focused onto a trifurcated optical fiber (core diameter: 600 μm, NA: 0.22). In some experiments, plasma saturation was observed. To mitigate this effect and prevent plasma saturation, neutral density transmission filters (optical densities: 0.3, 0.5, and 1) were positioned in front of the optical fiber. These filters attenuated the plasma emission to 50 %, 32 %, and 10 % of the original signal, respectively.

The optical fiber was connected to a three-channel Czerny-Turner spectrometer (Avantes ULS2048CL-EVO) equipped with CMOS technology, providing a spectral resolution of ~0.11 nm. The entrance slit was fixed at 10 μm. The spectrometer operated with a fixed delay time of 2 μs and an integration time of 2 ms, the justification for these settings are discussed in the following section.

The sampling position was adjusted using an XY stage and monitored with a Dino-Lite digital microscope. The number of laser pulses used depended on the specific sample and study requirements.

In this study, the electrode was placed at an angle of 60° relative to the propagation of the laser beam. The distance between the antenna and the sample was maintained at approximately 1 mm as the MW coupling was optimum. Previous studies have shown that the electromagnetic field generated by the antenna decays rapidly with distance, affecting the efficiency of microwave-plasma coupling and, consequently, the expansion and lifetime of the plasma [22,23]. Shorter distances, while beneficial for coupling, also imply practical limitations, such as the risk of physical contact and contamination of the antenna, as well as the need for frequent adjustments in heterogeneous samples with irregular surfaces. A contribution from the copper electrode was detected in the spectrum below 300 nm.

2.2. Spectrometer time parameters

Bibliographic research reveals that the spectra obtained by MW-LIBS exhibited similarities to those of conventional LIBS within the initial 1.5 microseconds, due to the high electron density of the plasmas (typically on the order of 10^{17} cm^{-3} [24,25]) Such a value is far above the critical cut-off density of 7×10^{10} cm^{-3} for 2.45 GHz microwave frequency [20,22,26]. Under these conditions, the plasma mainly reflects the

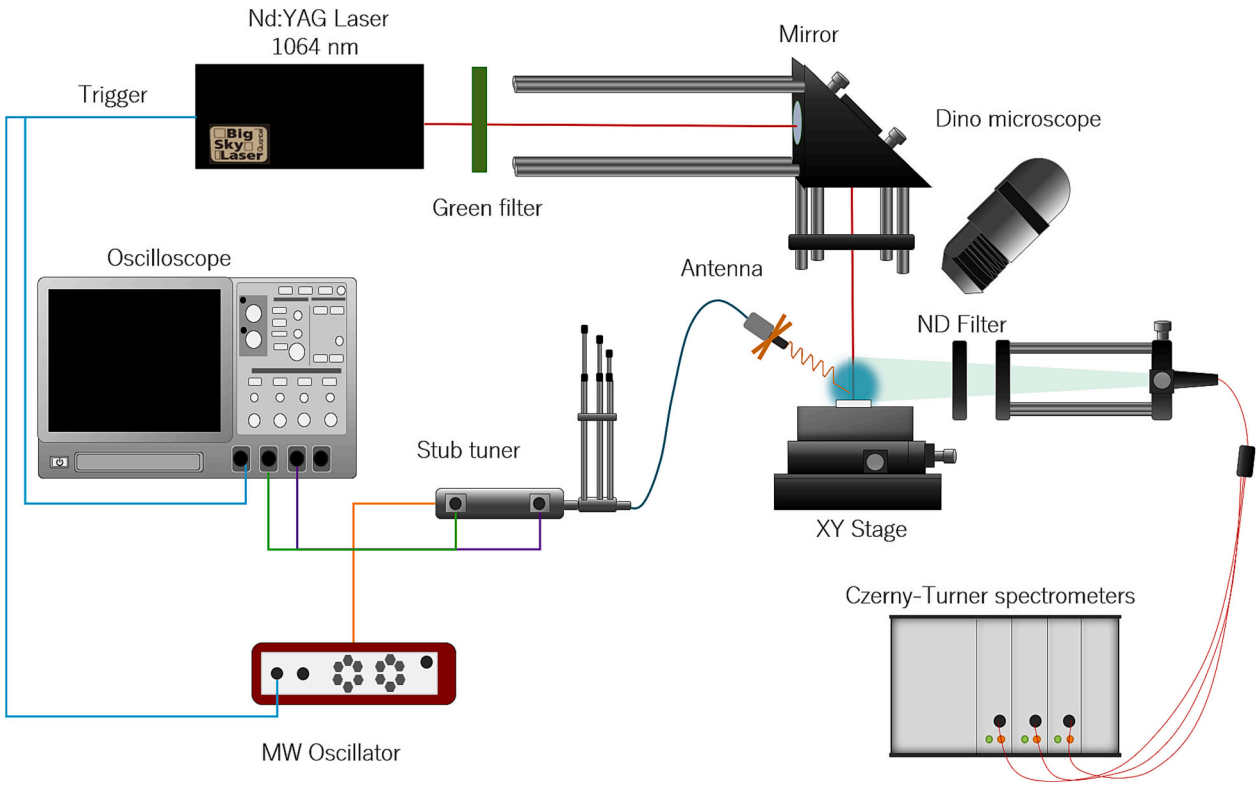

Fig. 1. A) Set-up for the MW-LIBS.

microwaves. Once the plasma cools down, the electron density decreases, enhancing the coupling of the microwave radiation [27,28]. Furthermore, as reported in the literature, the full width at half maximum (FWHM) of the emissions, which was initially broad at 0.56 nm, narrowed to a minimum value of 0.12 nm with delayed acquisition times exceeding 1.5 μs [20]. This time was confirmed by the time behavior of the forward and reflected power of the MW with the oscilloscope. Eventually, a delay of 2 μs was chosen between the laser pulse and the onset of spectral acquisition.

To ensure the complete integration of the microwave signal, the pulse duration for both LIBS and MW-LIBS was determined. A photodiode was utilized to collect the plasma signal, which was then monitored and recorded on an oscilloscope, the data are depicted in Fig. 2.

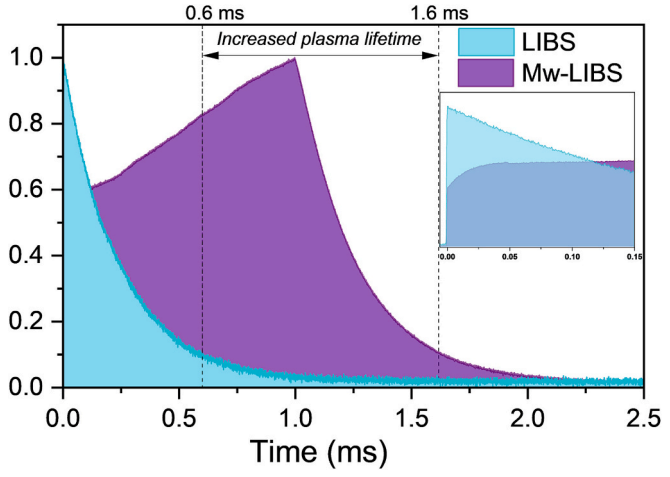

Fig. 2. Time comparison between LIBS and MW-LIBS normalized intensity decay on Al foil, average of 30 pulses, energy 5 mJ. MW parameter: 1 ms and 1 kW.

The criterion used to determine plasma duration was based on 10 % of the emitted plasma intensity relative to the maximum observed intensity. Aluminum foil was selected as the target for this conceptual test, as it is commonly employed in preliminary MW-LIBS studies due to its spectral simplicity, stability under repeated pulses, and suitability as a reference material [21, 26, 29]. As shown in Fig. 2, under the same conditions, an increase in plasma lifetime was observed in the aluminum foil, corresponding to the microwave pulse duration of 1 ms (MW-LIBS). The maximum intensity occured at the end of the microwave pulse (at 1 ms). This explains why the intensity continues to increase thereafter [30], compared to the conventional LIBS experiment. Additionally, both the plasma profile and peak were shifted, resulting in an increase in the area under the curve and a corresponding enhancement of the total signal.

Based on the obtained data, an integration time of 2 ms was selected. Although saturation issues were present, these were effectively addressed using neutral density filters, as previously described. Despite the saturation effects, a longer integration time was deemed preferable to ensure that the microwave effects were adequately captured and to observe their benefits in the formation of diatomic molecules detectable by LIBS.

2.3. Data analysis

The presence of microwaves influenced the emission intensity, with variations observed between measurements with and without microwaves. The microwave enhancement factor (EF) was quantified following Eq. (1).

$$EF = \frac{I_{MW-LIBS}}{I_{LIBS}}$$

This factor was determined by calculating the ratio of the MW-LIBS emission intensity $I_{MW\text{-}LIBS}$, to the corresponding emission intensity from the regular LIBS measurement I_{LIBS}.

3. Results and discussion

3.1. Enhancement molecular LIBS signal vs energy

Various studies have explored the behavior of LIBS and MW-LIBS signals in relation to laser energy. Conventional LIBS signal generally show a near-linear increase with laser energy, whereas MW-LIBS signals exhibit a less clear dependence, with high standard deviations beyond the plasma formation threshold, likely due to unstable microwave-plasma coupling efficiency [22,26].

In the present study, a graphite sample was analyzed by MW-LIBS. This substrate is well known, exhibits a spectrum particularly rich in molecular bands, and its transitions are well characterized and tabulated. As in previous research on atomic and ionic species, signal intensity did not show a significant increase or clear trend with higher laser energy. The results also extend this observation to molecular bands, which exhibited the same behavior, as shown in Fig. 3. The graphite samples showed a large enhancement factor which required the use of a neutral density filter to attenuate the overall signal detected. A threshold energy of 2.5 mJ was established for both LIBS and MW-LIBS, as this minimum energy is required to ensure sufficient plasma density for effective microwave coupling and to achieve the observed enhancement effect.

Regarding the molecular species identified in the graphite sample, it is dominated by CN and C_2. Although the sample has no nitrogen atoms, recombinations occur in the plasma between the fragmented carbon of the target and the nitrogen of the surrounding atmosphere that produce a strong emission of the CN radical.

Relative to the behavior of the sample during conventional LIBS analyses, at laser energies corresponding to the threshold of plasma formation, LIBS emissions are practically negligible. Only a weak signal corresponding to the CN violet system ($B^2\Sigma^+ \rightarrow X^2\Sigma^+$, $\Delta\nu = 0$) and to the most intense band (0–0) is detected. When microwave re-excitation (MW-LIBS) is applied, the spectrum changes substantially. Under the same energetic conditions, all major molecular emissions become clearly detectable, and their intensity increases by several orders of magnitude compared to conventional LIBS. This highlights the ability of microwave energy to sustain plasma and enhance molecule formation.

However, this enhancement does not occur uniformly across species. At a moderate laser energy of 5 mJ, the CN signals show a strong enhancement, whereas the behavior of the C_2 dimer is markedly different. The Swan system ($d^3\Pi g \rightarrow a^3\Pi u$, $\Delta\nu = +1$), associated with C_2,

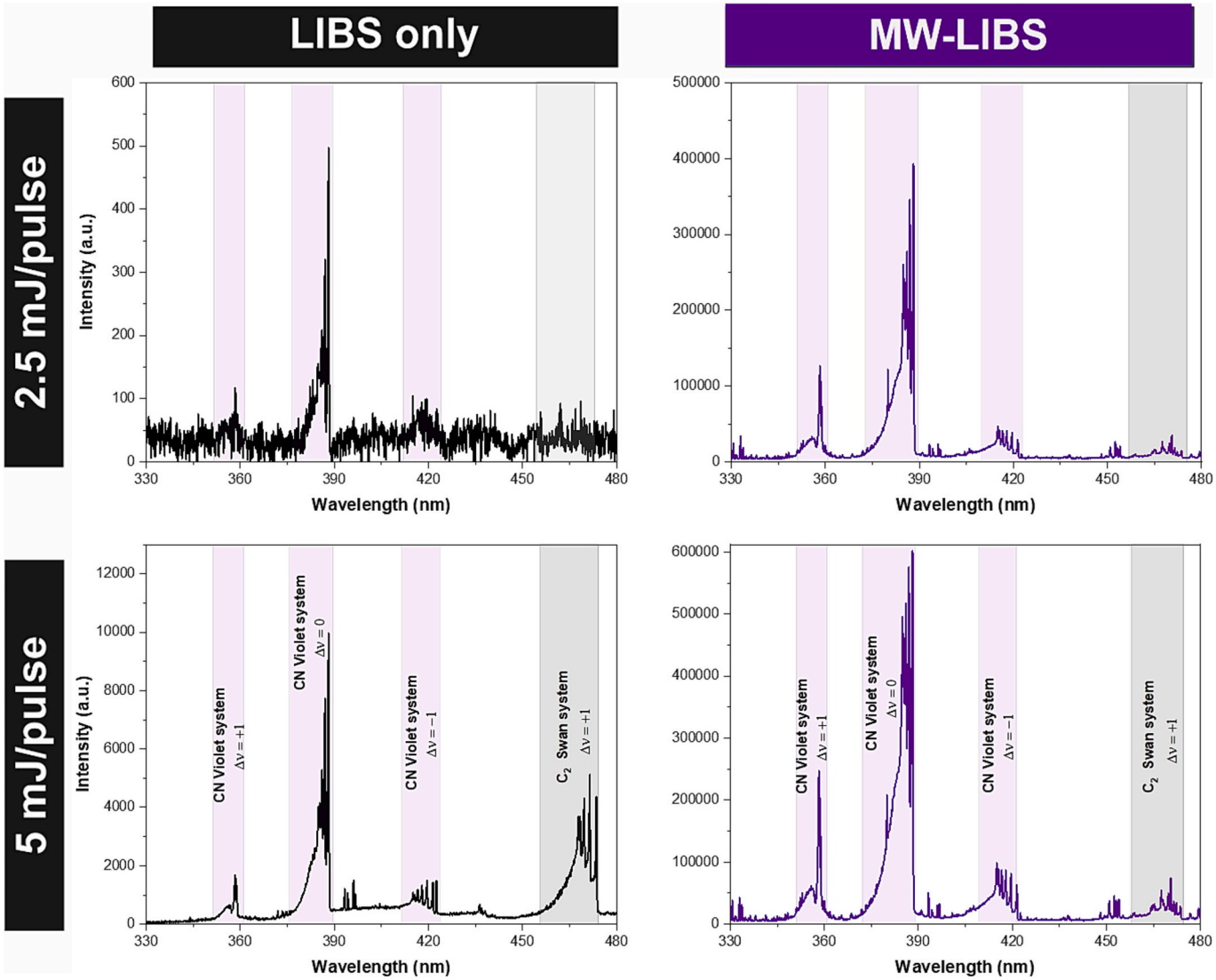

Fig. 3. Spectra recorded under LIBS-only (left column) and MW-assisted LIBS (right column) on graphite. The plots represent the average of 90 laser shots (30 spectra at 3 different sample locations). The experiments were performed at the energy threshold (E_{th} = 2.5 mJ/pulse) and twice this value ($2E_{th}$). The saturated Cu emission lines at 402.18 nm, 404.30 nm, 406.23 nm, 426.76 nm, 458.70 nm and 465.08 nm have been removed for clarity.

shows no significant enhancement beyond the plasma threshold. At higher fluences, the C_2 emission in MW-LIBS is even weaker than in standard LIBS. This behavior may be attributed to the prolonged plasma duration in MW-LIBS, which increases the interaction time of species within the plasma (electron impact, charged particle interactions, molecular excitation, dissociation, and recombination reactions) [31–33]. As a result, C_2 dissociates more easily, and free carbon tends to recombine into other molecular species such as CN, as shown in the following reactions.

$$C_2 \rightarrow 2C \ (607\ kJmol^{-1})$$

$$N_2 \rightarrow 2N \ (946\ kJ\ mol^{-1})$$

$$C + N \rightarrow CN$$

$$C + N_2 \rightarrow CN + N$$

$$C_2 + N_2 \rightarrow 2CN$$

An additional effect observed in the data is the spectral variability with respect to the input energy, showing no clear linear dependence. Fig. 4 presents the spectra associated with the CN transition ($B^2\Sigma^+ \rightarrow X^2\Sigma^+$), $\Delta\nu = +1$, and its most intense mode at 358.4 nm under conventional LIBS conditions and under MW-LIBS. The x-axis is represented in fluence thresholds multiple units, covering the range between 2.5 and 15 mJ/pulse. A value of 1 represents the minimum laser energy (in our case 2.5 mJ/pulse) required to record signal in the spectrograph.

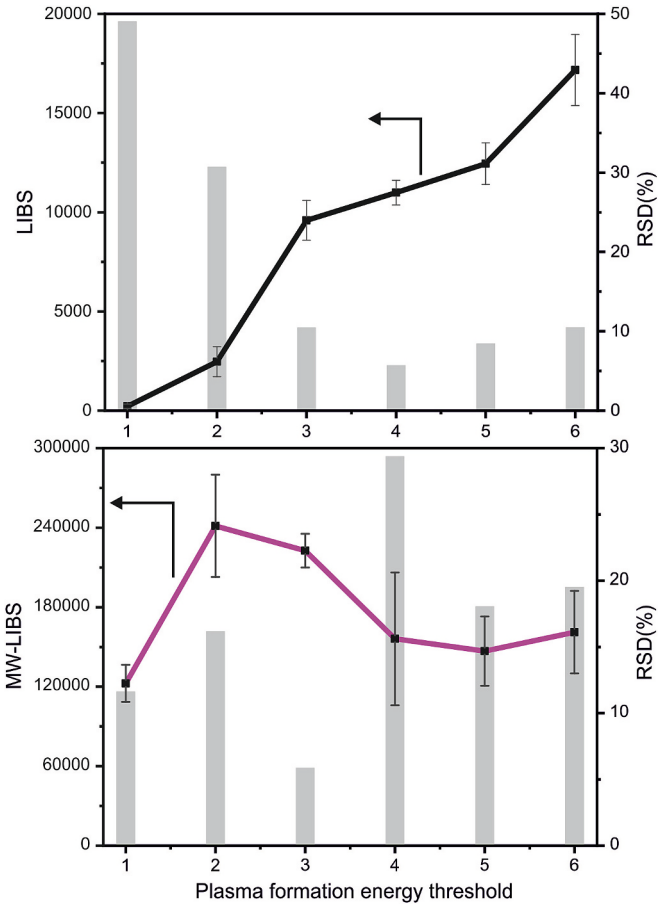

Fig. 4. Net intensities (line and dot plots) for the emission associated with the CN transition ($B^2\Sigma^+ \rightarrow X^2\Sigma^+$), $\Delta\nu = +1$, at its most intense mode (358.4 nm) for the LIBS only (top panel) and MW-LIBS (bottom panel) experiments. Each point represents the average of three positions and 30 pulses per position. The relative standard deviation (RSD) is shown as bars for each experiment. The enhancement factor at laser threshold values between 1 and 6 (corresponding to 2.5 to 15 mJ/pulse) is shown in the lower legend.

A higher standard deviation is observed in the MW-LIBS data, a trend that has been described in previous studies [22,23]. One study attributes large error bars at MW-LIBS to the instability of the initial plasma near the formation threshold [22], while the second study [23] identifies two regions in the calcium line intensity (422.7 nm) as a function of laser irradiance. In the low energy regime, efficient ablation was observed, with an increase in signal intensity along with irradiance. Above this threshold (50GW cm^{-2}), a shielding effect dominated, in which the high electron density plasma reflects the tail of the laser pulse, leading to signal saturation and increased inter-shot variability. This uncontrolled interaction amplifies shot-to-shot fluctuations, as shown by the large standard deviations in Fig. 4.

The enhancement factor of CN shows a substantial increase, reaching up to 559 times under threshold conditions. A noticeable change in slope was observed beyond three times the energy threshold (7.5 mJ), suggesting a transition in the enhancement behavior. These results highlight the advantage of operating near the energy threshold, where signal enhancement appears to be more effective, likely due to optimized plasma formation and interaction dynamics.

3.2. Signal amplification and broadened spectral access in MW-LIBS

One of the most significant advantages of MW-LIBS is its ability to generate significantly higher signal levels than traditional LIBS at the same laser pulse energy. MW-LIBS typically operates near the ablation threshold, achieving a substantial signal enhancement while utilizing reduced energy levels that minimize thermal and mechanical damage to the samples [29]. In the materials analyzed in this study, the pulse energy required for effective plasma generation ranged from 2.5 to 15 mJ, depending on the sample composition and physical properties [34–36].

Given this remarkable intensity enhancement, even at relatively low laser energies, the possibility of identifying molecular transitions that are well tabulated in the literature but rarely observed in conventional LIBS become feasible. This additional signal gain allows access to spectral regions that are typically less favored, not only due to the limitations of the detection system but also because of the inherently weak intensity of certain transitions. To this end, $CaCO_3$ in pellet form was selected for this analysis. The plasma generated leads to the formation of molecules of CaO, whose emission systems are known from the literature to extend across a broad portion of the LIBS spectral range.

In addition to the characteristic orange CaO emission system commonly observed in LIBS, an extreme red emission system $A^1\Sigma^+ \rightarrow X^1\Sigma^+$, was also detected, as shown in Fig. 5. Although the band heads of this system were reported by Pearse and Gaydon, specific vibrational transitions have not been conclusively identified in the literature [37].

This phenomenon may be due to the significant enhancement effect observed in MW-LIBS, which enable allows the identification of molecular species in the near-infrared region, that would typically remain undetectable under low-energy conditions. This extended spectral visibility offers a clear advantage, as the near-infrared region often exhibits fewer spectral interferences and provides another analytical window for molecular detection [38,39]. This effect increases the sensitivity and selectivity of MW-LIBS, which proves to be a powerful tool for trace analysis and complex sample characterization.

3.3. MW-LIBS for improved molecular emission detection

The conditions observed in MW-LIBS enhance the detection of molecular emissions, a trend highlighted in previous sections. In LIBS, the plasma is a reactive system, which facilitates the recombination of species from both the sample and the surrounding atmosphere. The use of microwaves amplifies this effect, promoting the formation of molecules that are unlikely to be seen in conventional LIBS.

The formation of molecular species in the plasma is strongly

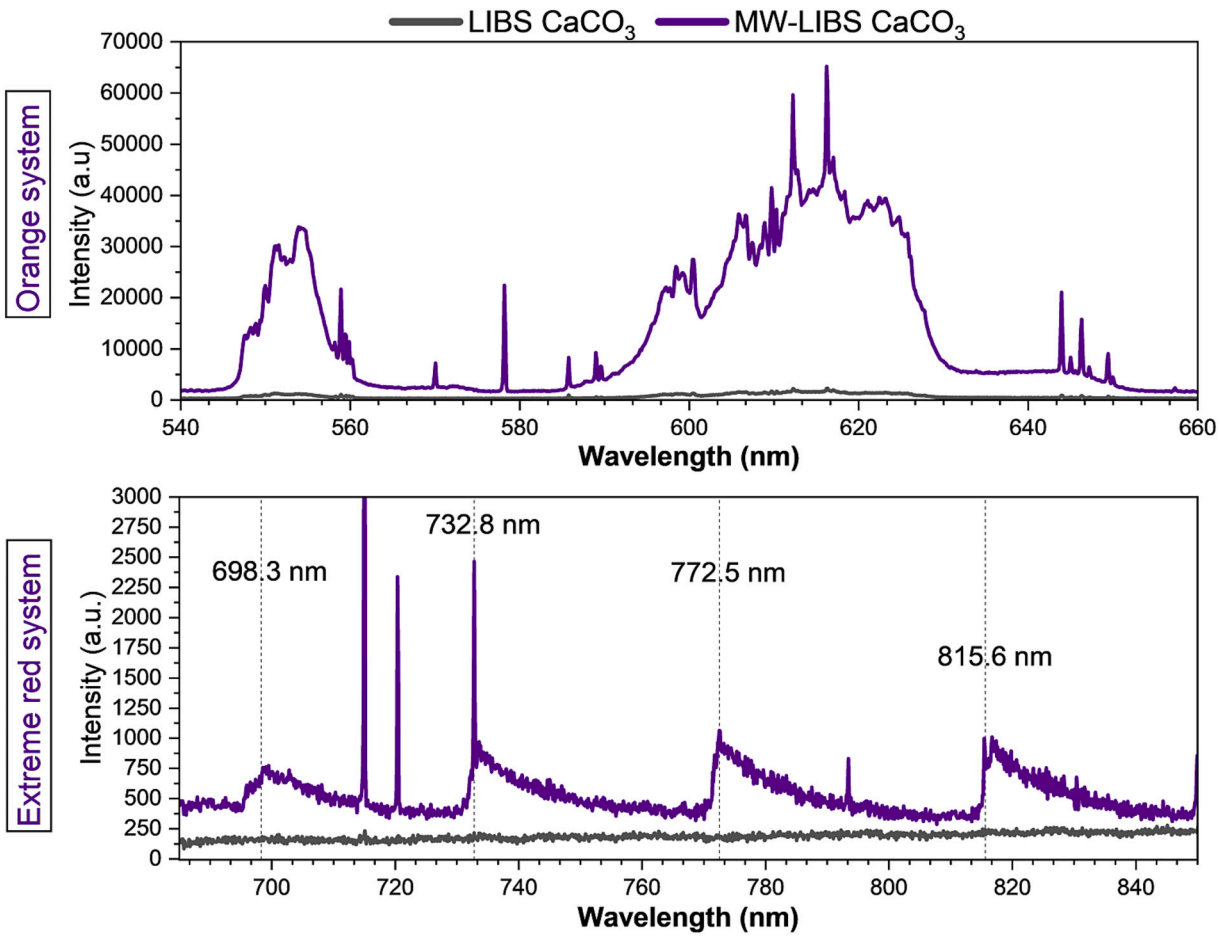

Fig. 5. Comparison between LIBS and MW-LIBS spectra of CaO, showing two spectral regions corresponding to the orange and extreme red emissions of the $A^1\Sigma^+ \rightarrow X^1\Sigma^{+system.}$ The laser was operated at the plasma formation threshold energy (4.5 mJ/pulse). Each spectrum represents the average of 50 laser shots. The intense discrete Cu emission lines from the electrode have been removed for better visualization. (For interpretation of the references to colour in this figure legend, the reader is referred to the web version of this article.)

influenced by the dissociation energy (D_0), which refers to the minimum energy required to separate the atoms in the ground state of the molecule. First, the temperature must be balanced: sufficiently high to support electronic excitation and, at the same time, low enough to enable molecular formation. Additionally, atomic reactants must be present at a sufficiently high density, particularly for reactions involving both the ablated material and the surrounding gas. Furthermore, it is imperative that the upper energy state is sufficiently low to permit electronic excitation [40].

Tin was selected as a test material because of its chemical versatility. It readily forms stable oxides under oxidizing conditions, while also being capable of producing volatile hydrides, albeit with limited stability. This dual reactivity increases the likelihood of generating transient molecular species in the plasma, making tin a suitable candidate for investigating whether the conditions established in MW-LIBS favor their persistence and subsequent spectroscopic detection.

The molecular emission of SnO was identified using MW-LIBS, a species typically not observed in conventional LIBS, illustrated in Fig. 6. This emission was specifically detected within the bands of the $D\ ^1\Pi \rightarrow X\ ^1\Sigma^+$ system. The spectral features at 338.83 nm, 341.58 nm, 348.45 nm, 358.54 nm, and 369.48 nm correspond to transitions described in Gaydon's reference for the main molecular spectrum system A [37]. Furthermore, additional emission lines, such as those at 361.47 nm and 372.12 nm, have also been identified, which is consistent with previous studies, including the work of Rajamanickam [41]. However, the observed system presents additional complexity due to the presence of

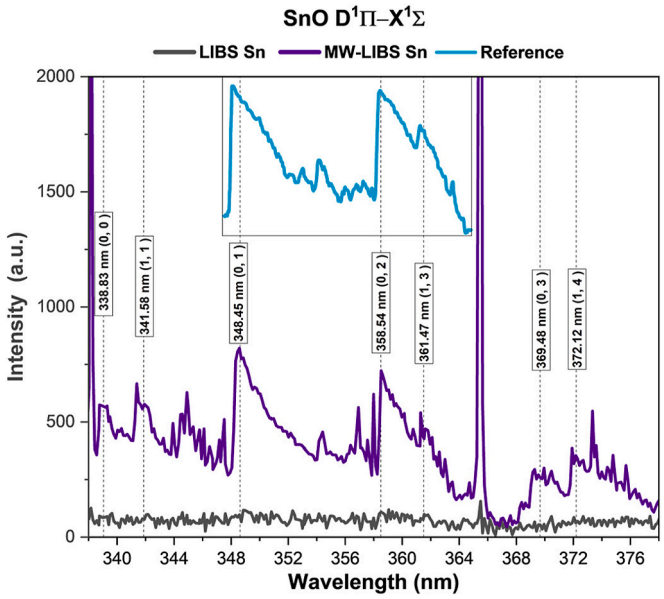

Fig. 6. The figure presents the $D^1\Pi \rightarrow X^1\Sigma^+$ system A of SnO, combining experimental spectra obtained using LIBS and MW-LIBS with reference data adapted from Rajamanickam [46]. The measurements were taken from a single laser shot at 5 mJ, corresponding to twice the threshold energy.

intense atomic and ionic tin lines within the 300.91–380.10 nm region, which can overlap with molecular emissions.

The preferential formation of SnO in MW-LIBS could be explained by considering the energy levels associated with the D $^1\Pi \rightarrow$ X $^1\Sigma^+$ system, which has a primary excitation energy around 3.56 eV (calculated). While this energy range is accessible in conventional LIBS, SnO formation is not typically observed, suggesting additional limiting factors. One possible explanation is the restricted availability of Sn and O species in the plasma, as molecular recombination requires a sufficiently dense oxygen environment. In MW-LIBS, the larger plasma dimension may help overcome this limitation [42]. A more extensive interaction with ambient oxygen increases the availability of O species for recombination.

Furthermore, the efficiency of SnO formation is influenced by plasma collision dynamics, where the probability of effective recombination depends on the plasma conditions. A possible explanation for the preferential formation of molecular bands is that, as the plasma expands and cools, recombination processes become more favorable. When the temperature drops sufficiently, collisions between heavy particles (atoms and ions) dominate over electronic interactions, promoting molecular species formation [40].

Another relevant factor is the moderate dissociation energy of SnO (5.4 eV) [43], which may make it more prone to thermal fragmentation in the high-temperature plasma core of conventional LIBS. In contrast, diatomic species such as the cyanogen radical (CN) and nitrogen dimer (N_2), with higher dissociation energies (>7 eV), are more resistant to decomposition and therefore more readily detected in LIBS [40,44,45].

4. Conclusions

The results of this study show that the use of MW-LIBS leads to a plasma regime that differs from that generated by conventional LIBS. This regime creates conditions that favor the preservation of molecular species in the plasma, thereby improving their detectability. The analyses revealed that microwave re-excitation extended the plasma lifetime to approximately 2 milliseconds, representing a significant increase compared to conventional LIBS under similar energy conditions. This longer duration is one of the main factors contributing to the observed signal enhancement.

Experiments performed on the violet system of the CN radical ($B^2\Sigma^+ \rightarrow X^2\Sigma^+$, $\Delta\nu = 0$, 358.4 nm) at different laser energy inputs indicated that the most favorable conditions for detection occurred near the plasma formation threshold. The degree of signal enhancement was also found to depend on the molecular species involved, highlighting the importance of investigating the formation mechanisms of each species individually. In the case of the graphite sample, the CN/C_2 ratio was significantly higher in MW-LIBS, suggesting enhanced CN formation promoted by interactions between the plasma and atmospheric nitrogen. This effect may be attributed to the larger plume volume and increased collision frequency with the ambient gas.

Although MW-LIBS generally exhibited higher standard deviations compared to conventional LIBS, these values were considerably lower under threshold energy conditions. This observation suggests improved plasma stability and more uniform behavior under such circumstances. The enhancement in emission intensity induced by microwave coupling also helped to overcome instrumental limitations in the infrared region of the spectrum. As a result, emissions from the extreme red system of CaO ($A^1\Sigma^+ \rightarrow X^1\Sigma^+$) in the near-infrared were successfully detected. These emissions are typically not observed in conventional LIBS due to the low sensitivity of detectors in that spectral range.

An additional finding was the identification of the SnO fragment ($D^1\Pi \rightarrow X^1\Sigma^+$) in a tin sample, which has not been previously reported using LIBS. This result may be explained by the increased number of collisions promoted by microwave re-excitation, as well as by the conditions that favor the recombination of species formed in both the plasma and the surrounding atmosphere.

Although these are preliminary results, they highlight the potential of MW-LIBS as a reliable and adaptable tool for improving the detection of molecular species. These findings provide a solid basis for further investigation of MW-LIBS, with particular attention to its applicability across different types of samples and environmental conditions. Exploring these aspects in greater detail may help elucidate the mechanisms responsible for signal enhancement and the selective formation of molecular species. Notably, the increased reactivity of microwave-sustained plasma, relative to conventional LIBS, could promote the formation of specific molecular fragments and expand the range of detectable species through their molecular band emissions.

CRediT authorship contribution statement

L. García-Gómez: Writing – review & editing, Writing – original draft, Visualization, Methodology, Data curation. **J.K. Soriano:** Writing – review & editing. **J.M. Vadillo:** Writing – review & editing, Supervision, Conceptualization. **Y. Ikeda:** Writing – review & editing, Supervision, Methodology.

Declaration of competing interest

None.

Acknowledgements

This work was supported by Programa Operativo FEDER Andalucía 2014–2020, Consejería de Economía y Conocimiento de la Junta de Andalucía, Reference UMA18-FEDERJA-272 and by Project PID2020-119185GB-I00 from the Ministerio de Economia y Competitividad of Spain. An author, L. García-Gómez, is grateful to the Spanish Ministerio de Economia y Competitividad for the concession of a FPI grant from Project PID2020-119185GB-I00.

Data availability

Data will be made available on request.

References

[1] F.J. Fortes, J. Moros, P. Lucena, L.M. Cabalín, J.J. Laserna, Laser-induced breakdown spectroscopy, Anal. Chem. 85 (2013) 640–669, https://doi.org/10.1021/ac303220r.
[2] R. Gaudiuso, M. Dell'Aglio, O.D. Pascale, G.S. Senesi, A.D. Giacomo, Laser induced breakdown spectroscopy for elemental analysis in environmental, cultural heritage and space applications: a review of methods and results, Sensors 10 (2010) 7434–7468, https://doi.org/10.3390/s100807434.
[3] J. Laserna, J.M. Vadillo, P. Purohit, Laser-induced breakdown spectroscopy (LIBS): fast, effective, and agile leading edge analytical technology, Appl. Spectrosc. 72 (2018) 35–50, https://doi.org/10.1177/0003702818791926.
[4] D.W. Hahn, N. Omenetto, Laser-induced breakdown spectroscopy (LIBS), part II: review of instrumental and methodological approaches to material analysis and applications to different fields, Appl. Spectrosc. 66 (2012) 347–419, https://doi.org/10.1366/11-06574.
[5] S.J. Chen, A. Iqbal, M. Wall, C. Fumeaux, Z.T. Alwahabi, Design and application of near-field applicators for efficient microwave-assisted laser-induced breakdown spectroscopy, J. Anal. At. Spectrom. 32 (2017) 1508–1518, https://doi.org/10.1039/C7JA00046D.
[6] A. De Giacomo, R. Gaudiuso, M. Dell'Aglio, A. Santagata, The role of continuum radiation in laser induced plasma spectroscopy, Spectrochim. Acta B At. Spectrosc. 65 (2010) 385–394, https://doi.org/10.1016/j.sab.2010.03.016.
[7] L.J. Radziemski, T.R. Loree, Laser-induced breakdown spectroscopy: time-resolved spectrochemical applications, Plasma Chem. Plasma Process. 1 (1981) 281–293, https://doi.org/10.1007/BF00568836.
[8] A. De Giacomo, M. Dell'Aglio, D. Bruno, R. Gaudiuso, O. De Pascale, Experimental and theoretical comparison of single-pulse and double-pulse laser induced breakdown spectroscopy on metallic samples, Spectrochim. Acta B At. Spectrosc. 63 (2008) 805–816, https://doi.org/10.1016/j.sab.2008.05.002.
[9] R. Noll, R. Sattmann, V. Sturm, S. Winkelmann, Space- and time-resolved dynamics of plasmas generated by laser double pulses interacting with metallic samples, J. Anal. At. Spectrom. 19 (2004) 419–428, https://doi.org/10.1039/B315718K.
[10] B. Rashid, R. Ahmed, R. Ali, M.A. Baig, A comparative study of single and double pulse of laser induced breakdown spectroscopy of silver, Phys. Plasmas 18 (2011), https://doi.org/10.1063/1.3599591.

[11] A.S. Zakuskin, A.M. Popov, S.M. Zaytsev, N.B. Zorov, M.V. Belkov, T.A. Labutin, Orthogonal and collinear configurations in double-pulse laser-induced breakdown spectrometry to improve sensitivity in chlorine determination, J. Appl. Spectrosc. 84 (2017) 319–323, https://doi.org/10.1007/s10812-017-0470-y.
[12] M. Weidman, M. Baudelet, S. Palanco, M. Sigman, P.J. Dagdigian, M. Richardson, Nd:YAG-CO2 double-pulse laser induced breakdown spectroscopy of organic films, Opt. Express 18 (2010) 259–266, https://doi.org/10.1364/OE.18.000259.
[13] L.B. Guo, Z.H. Zhu, J.M. Li, Y. Tang, S.S. Tang, Z.Q. Hao, X.Y. Li, Y.F. Lu, X.Y. Zeng, Determination of boron with molecular emission using laser-induced breakdown spectroscopy combined with laser-induced radical fluorescence, Opt. Express 26 (2018) 2634–2642, https://doi.org/10.1364/OE.26.002634.
[14] J. Li, Z. Zhu, R. Zhou, N. Zhao, R. Yi, X. Yang, X. Li, L. Guo, X. Zeng, Y. Lu, Determination of carbon content in steels using laser-induced breakdown spectroscopy assisted with laser-induced radical fluorescence, Anal. Chem. 89 (2017) 8134–8139, https://doi.org/10.1021/acs.analchem.7b01932.
[15] L. Nagli, M. Gaft, Y. Raichlin, Halogen detection with molecular laser induced fluorescence, Spectrochim. Acta B At. Spectrosc. 166 (2020) 105813, https://doi.org/10.1016/j.sab.2020.105813.
[16] M. Gaft, L. Nagli, A. Gorychev, Y. Raichlin, High-resolution LIBS and LIBS-MLIF of REE molecular emission in laser-induced plasma, Spectrochim. Acta B At. Spectrosc. 204 (2023) 106667, https://doi.org/10.1016/j.sab.2023.106667.
[17] X.K. Shen, H. Wang, Z.Q. Xie, Y. Gao, H. Ling, Y.F. Lu, Detection of trace phosphorus in steel using laser-induced breakdown spectroscopy combined with laser-induced fluorescence, Appl. Opt. 48 (2009) 2551–2558, https://doi.org/10.1364/AO.48.002551.
[18] H.H. Telle, D.C.S. Beddows, G.W. Morris, O. Samek, Sensitive and selective spectrochemical analysis of metallic samples: the combination of laser-induced breakdown spectroscopy and laser-induced fluorescence spectroscopy, Spectrochim. Acta B At. Spectrosc. 56 (2001) 947–960, https://doi.org/10.1016/S0584-8547(01)00190-2.
[19] S.S. Harilal, N.L. LaHaye, M.C. Phillips, High-resolution spectroscopy of laser ablation plumes using laser-induced fluorescence, Opt. Express 25 (2017) 2312–2326, https://doi.org/10.1364/OE.25.002312.
[20] Y. Ikeda, J.K. Soriano, I. Wakaida, Signal-to-noise ratio improvements in microwave-assisted laser-induced breakdown spectroscopy, Talanta Open 6 (2022) 100138, https://doi.org/10.1016/j.talo.2022.100138.
[21] Y. Ikeda, Y. Hirata, J.K. Soriano, I. Wakaida, Antenna characteristics of helical coil with 2.45 GHz semiconductor microwave for microwave-enhanced laser-induced breakdown spectroscopy (MW-LIBS), Materials 15 (2022) 2851, https://doi.org/10.3390/ma15082851.
[22] J. Viljanen, Z. Sun, Z.T. Alwahabi, Microwave assisted laser-induced breakdown spectroscopy at ambient conditions, Spectrochim. Acta B At. Spectrosc. 118 (2016) 29–36, https://doi.org/10.1016/j.sab.2016.02.002.
[23] M. Oba, M. Miyabe, K. Akaoka, I. Wakaida, Development of microwave-assisted, laser-induced breakdown spectroscopy without a microwave cavity or waveguide, Jpn. J. Appl. Phys. 59 (2020) 062001, https://doi.org/10.35848/1347-4065/ab8b3f.
[24] P.K. Diwakar, D.W. Hahn, Study of early laser-induced plasma dynamics: transient electron density gradients via Thomson scattering and stark broadening, and the implications on laser-induced breakdown spectroscopy measurements, Spectrochim. Acta B At. Spectrosc. 63 (2008) 1038–1046, https://doi.org/10.1016/j.sab.2008.07.003.
[25] E. Tognoni, G. Cristoforetti, S. Legnaioli, V. Palleschi, Calibration-free laser-induced breakdown spectroscopy: state of the art, Spectrochim. Acta B At. Spectrosc. 65 (2010) 1–14, https://doi.org/10.1016/j.sab.2009.11.006.
[26] Y. Liu, M. Baudelet, M. Richardson, Elemental analysis by microwave-assisted laser-induced breakdown spectroscopy: evaluation on ceramics, J. Anal. At. Spectrom. 25 (2010) 1316–1323, https://doi.org/10.1039/C003304A.
[27] M. Tampo, M. Miyabe, K. Akaoka, M. Oba, H. Ohba, Y. Maruyama, I. Wakaida, Enhancement of intensity in microwave-assisted laser-induced breakdown spectroscopy for remote analysis of nuclear fuel recycling, J. Anal. At. Spectrom. 29 (2014) 886–892, https://doi.org/10.1039/C3JA50259G.
[28] Y. Ikeda, J.K. Soriano, H. Ohba, I. Wakaida, Laser ablation plasma expansion using microwaves, Sci. Rep. 13 (2023) 13901, https://doi.org/10.1038/s41598-023-41208-z.
[29] Y. Ikeda, J.K. Soriano, I. Wakaida, Interactions of microwaves with alumina surface in microwave-enhanced laser-induced breakdown spectroscopy, Opt. Laser Technol. 159 (2023) 108982, https://doi.org/10.1016/j.optlastec.2022.108982.
[30] Y. Fan, Y. Gu, Z. Hu, F. Chen, J. Nie, Y. Liu, W. Cheng, L. Guo, Self-reversal effect elimination in laser-induced breakdown spectroscopy by employing single-probe microwave radiation, J. Anal. At. Spectrom. 38 (2023) 1713–1719, https://doi.org/10.1039/D3JA00098B.
[31] M.A. Wakil, Z.T. Alwahabi, Quantitative fluorine and bromine detection under ambient conditions via molecular emission, J. Anal. At. Spectrom. 35 (2020) 2620–2626, https://doi.org/10.1039/D0JA00200C.
[32] A. Khumaeni, K. Akaoka, M. Miyabe, I. Wakaida, The role of microwaves in the enhancement of laser-induced plasma emission, Front. Phys. 11 (2016) 114209, https://doi.org/10.1007/s11467-016-0581-6.
[33] M.A. Wakil, Z.T. Alwahabi, Microwave-assisted laser induced breakdown molecular spectroscopy: quantitative chlorine detection, J. Anal. At. Spectrom. 34 (2019) 1892–1899, https://doi.org/10.1039/C9JA00151D.
[34] P.R. Villas-Boas, M.A. Franco, L. Martin-Neto, H.T. Gollany, D.M. Milori, Applications of laser-induced breakdown spectroscopy for soil analysis, part I: review of fundamentals and chemical and physical properties, Eur. J. Soil Sci. 71 (2020) 789–804, https://doi.org/10.1111/ejss.12889.
[35] V.N. Rai, S.N. Thakur, Chapter 4 - physics and dynamics of plasma in laser-induced breakdown spectroscopy, in: J.P. Singh, S.N. Thakur (Eds.), Laser-Induced Breakdown Spectroscopy, Second edition, Elsevier, Amsterdam, 2020, pp. 71–106, https://doi.org/10.1016/B978-0-12-818829-3.00004-6.
[36] T.L. Thiem, Y.-I. Lee, J. Sneddon, Lasers in atomic spectroscopy: selected applications, Microchem. J. 45 (1992) 1–35, https://doi.org/10.1016/0026-265X(92)90067-D.
[37] R.W.B. Pearse, A.G. Gaydon, R.W.B. Pearse, A.G. Gaydon, The Identification of Molecular Spectra, Chapman and Hall London, 1976.
[38] G. Asimellis, S. Hamilton, A. Giannoudakos, M. Kompitsas, Controlled inert gas environment for enhanced chlorine and fluorine detection in the visible and near-infrared by laser-induced breakdown spectroscopy, Spectrochim. Acta B At. Spectrosc. 60 (2005) 1132–1139, https://doi.org/10.1016/j.sab.2005.05.035.
[39] C.S.C. Yang, E.E. Brown, U. Hommerich, F. Jin, S.B. Trivedi, A.C. Samuels, A. P. Snyder, Long-wave, infrared laser-induced breakdown (LIBS) spectroscopy emissions from energetic materials, Appl. Spectrosc. 66 (2012) 1397–1402, https://doi.org/10.1366/12-06700.
[40] A. De Giacomo, J. Hermann, Laser-induced plasma emission: from atomic to molecular spectra, J. Phys. D. Appl. Phys. 50 (2017) 183002, https://doi.org/10.1088/1361-6463/aa6585.
[41] N. Rajamanickam, Intensity distribution in the bands of the D 1 Π→ X 1 Σ+ system of SnO, Pramana 25 (1985) 179–186, https://doi.org/10.1007/BF02847657.
[42] D. Diaz, D.W. Hahn, Plasma chemistry produced during laser ablation of graphite in air, argon, helium and nitrogen, Spectrochim. Acta B At. Spectrosc. 166 (2020) 105800, https://doi.org/10.1016/j.sab.2020.105800.
[43] R. Colin, J. Drowart, G. Verhaegen, Mass-spectrometric study of the vaporization of tin oxides. Dissociation energy of SnO, Trans. Faraday Soc. 61 (1965) 1364–1371, https://doi.org/10.1039/TF9656101364.
[44] A.D. Pradhan, H. Partridge, C.W. Bauschlicher Jr., The dissociation energy of CN and C2, J. Chem. Phys. 101 (1994) 3857–3861, https://doi.org/10.1063/1.467503.
[45] A.G. Gaydon, W.G. Penney, The dissociation energies of CO, N2, NO and CN, Proc. Roy. Soc. Lond. Ser. A. Math. Phys. Sci. 183 (1945) 374–388.